Theory of Raman scattering with final-state interaction in high-T_c BCS superconductors: Collective modes

H. Monien and A. Zawadowski*
Department of Physics, University of Illinois at Urbana-Champaign, 1110 West Green Street, Urbana, Illinois 61801
(Received 4 December 1989)

A theory of Raman scattering in isotropic superconductors is presented, where the light breaks a Cooper pair. The role of the final-state interaction including the long-range Coulomb interaction is discussed in great detail. It is shown that the Raman spectrum consists of two parts: bound states with different symmetries below the threshold ($\omega < 2\Delta$) and a continuum above the threshold, where the square-root singularity is removed by the final-state interaction. The small binding energies of the bound states cannot be resolved because of the experimental broadening and the possible lifetime (recombination time) of the excited pair. The spectrum shows very weak dependence on the momentum transfer providing that the transfer q is not too large thus $q \ll \Delta/v_F$. The spectrum is sensitive, however, on the polarizations of the incident and scattered light, because the relative weights of the excited pairs with different symmetries are also sensitive. It is also demonstrated that it is not necessary to invoke a large gap anisotropy to explain a broadening of the pair breaking edge at 2Δ. The results previously derived by Klein and Dierker and by Abrikosov and Falkovsky are also discussed. The present results agree with the former ones in the zero momentum transfer limit, while the later ones are reproduced for small momentum transfer in certain energy regions.

I. INTRODUCTION

Following the BCS (Ref. 1) theory of superconductivity Anderson[2,3] and Bogoliubov,[4] in their classic papers of 1958, called attention to the existence of collective excitation in superconductors. One of the modes is the plasma mode and the other collective excitations are bound pairs of single-particle excitations orthogonal to the Cooper pairs that lie near the gap edge 2Δ. Following these papers Tsuneto[5] and also Bardasis and Schrieffer[6] carried out extensive studies of the bound pairs, with the latter authors especially providing a very detailed description. The basic physical idea is that when a Cooper pair is excited to two single excitations then the so-called residual interaction between these excitations, which does not contribute to the Cooper-pair formation, results in other bound pairs orthogonal to the Cooper pair. Assuming that the new pairs have approximately zero total momentum, then their angular momenta must be different from zero ($l \neq 0$). It also was shown that static impurities shift the energy of the pair but the damping is not appreciable.[7] When the first experimental attempts to find these excitations in infrared absorption spectra failed,[8] general interest in these excitations almost disappeared, except in superfluid ^{3}He.[9] It is interesting to note that there was no early study to show how the residual interaction modifies the two-excitation continuum.

The two-excitation spectra are, however, measurable by Raman scattering. The first theoretical work is due to Abrikosov and Fal'kovskii,[10] where the final-state interaction has already been discussed, but no attention was paid to the formation of bound pairs. Such experimental studies became feasible by the development of laser spectroscopy, as was first pointed out by Tong and Maradudin.[11] The first clear evidence for the existence of the superconducting gap in the Raman spectra was given by Sooryakumar and Klein,[12] studying $2H$-$NbSe_2$. Bardeen[13] has pointed out for us that the interaction between two single excitations may play a role in the temperature dependence of the nuclear-spin-relaxation time in superconductors (coherence peak).

There is, however, another physical example of the two excitation bound states that are the two-roton excitations generated by Raman scattering in liquid ^{4}He, where the two free rotons also have a density of states with square-root singularities as in superconductors. For attractive roton-roton interaction two-roton bound states are formed and the continuum spectrum is essentially modified and also disappears at the threshold, as shown in Fig. 1(a). In the measurements of Greytak and coworkers[14] the bound state has never been resolved; instead a similar curve, shown by the dashed line in Fig. 1(b), has been measured. Fitting the measured Raman spectra by theoretical prediction,[15–17] the roton-roton coupling strength and the single-roton energy was determined.[18] The obtained roton energy was later verified by neutron-scattering measurements.[19]

There is a striking similarity between the measured Raman spectra in A-15 compounds and the spectra of two-roton excitations. There is, however, an essential difference between these cases, namely, the roton dispersion in liquid ^{4}He is completely isotropic, while in the superconductive gap there is always some anisotropy due to the crystal lattice even in the BCS state. Previously, the smearing of the singularity at the threshold has been mainly attributed to the anisotropy rather than to final-state interaction.[20,21] The main goal of this paper is to point out that it is not a trivial task to differentiate between anisotropy and final-state interaction.

There is a further difference between the roton and su-

 ©1990 The American Physical Society

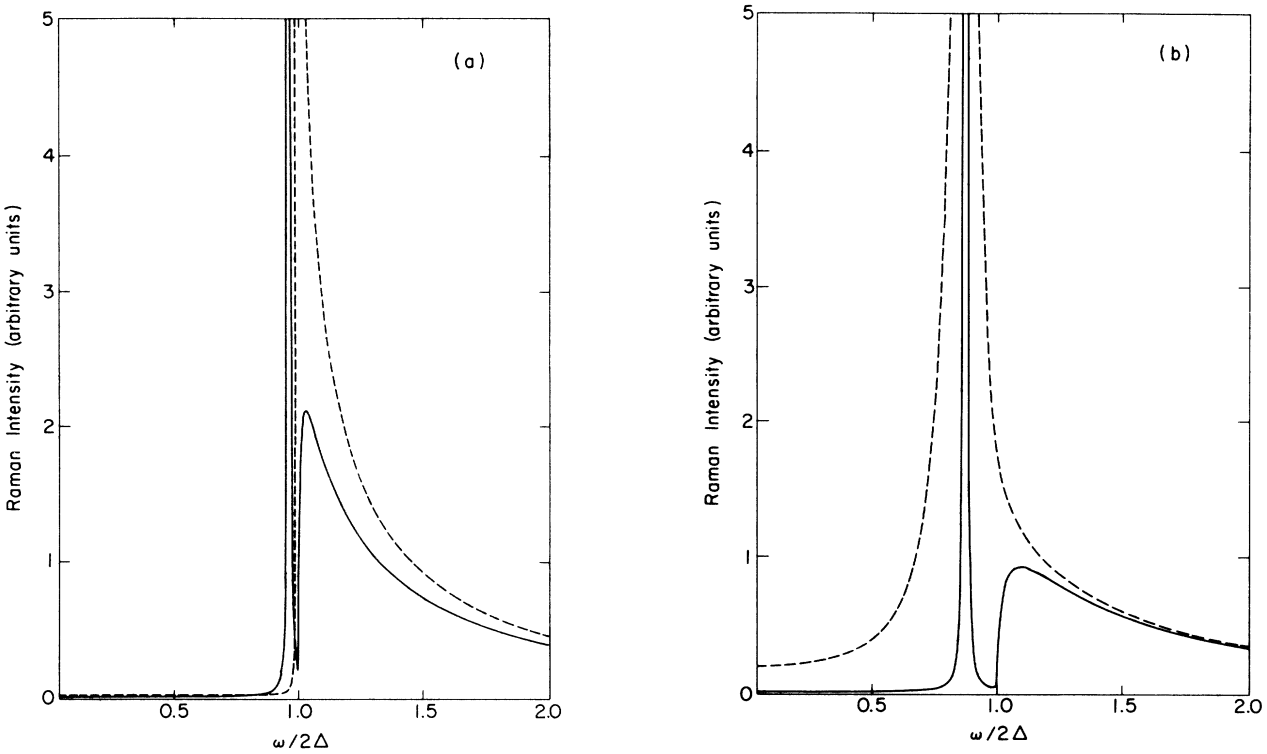

FIG. 1. Typical spectra of Raman scattering by two excitations: (a) The dashed line corresponds to the case of weakly interacting excitations ($\alpha=0.01$) and the solid line indicates the effect of attractive effective interaction between the excitations ($\alpha=0.1$). (b) The effect of Lorentzian broadening due to experimental resolution or finite life (recombination) time of the pair excitation is shown for two values of the broadening Γ ($\Gamma=1\times10^{-3}$ solid line, $\Gamma=1\times10^{-2}$ dashed line). The value of $\alpha=0.2$ is used in (b). In the case of larger broadening the bound state cannot be resolved, but the spectrum is shifted to lower energies. The Lorentzian broadening may be responsible for the artificially long tail of the spectrum at the low-energy side.

perconducting case. As Bardasis and Schrieffer pointed out,[6] the bound state is formed in superconductors for an arbitrary sign of the coupling and, depending on the sign, the bound pair has mostly a two-electron or electron-hole pair character.

Recently, the new experimental data on A-15 compounds[20–23] attracted the new interest of Klein and Dierker[21] in the final-state interaction, which was followed by the work of Abrikosov and Fal'kovskii,[24] stimulated by the discovery of high-temperature superconductivity. The theory of Klein and Dierker's[21] covered the whole energy spectrum, while the former authors concentrated on different limits. It will be shown that the two theories are not contradictory, but that very different questions have been asked.

These recent theories address those materials in which the size of the Cooper pair given by the BCS coherence length ξ_0 is small compared to the penetration depth δ of the light into the material ($\xi_0 \ll \delta$). Simple metals with weak BCS coupling belong to the opposite group ($\xi_0 > \delta$), where the excited pairs do not have negligible total momenta. In the latter case that average over the momenta $\mathbf{q}$, must be taken, thus the characteristic features can be less transparent. By Raman scattering, in principle, both of the different types of collective excitations can be studied.

(i) Pairs of excitations which are in $l=0$, s state and represent long-wavelength density oscillations are coupled to the Coulomb field. As it will be shown, in this case the Raman spectrum is very weak, as it is proportional to $q^2 v_F^2/\omega_p^2$ where q is the momentum transfer, v_F is Fermi velocity, and ω_p is the plasma frequency. This problem was first studied by Abrikosov and Genkin,[25]

(ii) Pairs orthogonal to the Cooper pairs can be characterized by $l\neq0$ angular momentum or by different crystal harmonics. These excitations do not carry net charge, thus they are not coupled to long-range Coulomb fields. In this study, these states are characterized by different quantum numbers L, and for simplicity there is no mixing between the different L channels. The relative weights of these channels in the Raman spectra are determined by the polarizations of the incident and scattered light ($\mathbf{e}_i$ and $\mathbf{e}_s$).

In this paper, a complete study of the Raman spectrum in BCS superconductors is presented. In Sec. II, the general formalism is presented. Section III is devoted to the study of the vertex equations and the solution in order to describe the residual interaction in the final state. In Sec. IV, the different results are discussed separately. In Part A, first the bound states in the gap and then the continua

are studied in the zero total momentum limit ($q=0$). In Part B, the small q case is discussed, focusing on the coupling between density and the plasma oscillations, and on the q dependence of the excitations that do not carry net charge. The results obtained are summarized in Sec. V. Appendixes A, B, and C contain the mathematical details.

II. GENERAL FORMALISM

In this paper the finite temperature Green's function technique[26] will be applied to make further generalizations more straightforward. For the sake of simplicity, the final results will be given for zero temperature.

A. Raman scattering

The energies, momenta, and polarization directions of the incident and scattered light are denoted by $\omega_i,\mathbf{k}_i,\mathbf{e}_i$ and $\omega_s,\mathbf{k}_s,\mathbf{e}_s$; furthermore, the energy and momentum transfer to the material are $\omega=\omega_i-\omega_s$ and $\mathbf{q}=\mathbf{k}_i-\mathbf{k}_s$. For A-15 compounds and high-T_c superconductors the penetration depth of the light into the material δ is large ($\delta\sim 180$ Å for Nb_3Sn and $\delta<1000$ Å for high T_c materials); therefore, the momentum transfer $\mathbf{q}$ is small compared to the inverse of the BCS coherence length, and thus $qv_F/\Delta\ll 1$, where $\mathbf{v}_F$ is the Fermi velocity.

The Raman scattering can be treated as a scattering on an effective density $\tilde{\rho}_\mathbf{q}$

$$\tilde{\rho}_\mathbf{q}=\sum_{\mathbf{k},\sigma}\gamma_\mathbf{k}a^\dagger_{\mathbf{k}+\mathbf{q},\sigma}a_{\mathbf{k},\sigma}\ , \tag{2.1}$$

where $a_{\mathbf{k},\sigma}$ is the annihilation operator of the electron with momentum $\mathbf{k}$ and spin σ ($\sigma=\pm1$) in the single conduction band treated, and $\gamma_\mathbf{k}$ gives the strength of the scattering, which has the form

$$\gamma_\mathbf{k}=(\mathbf{e}_i\cdot\mathbf{e}_s)+m^{-1}\sum_b\left[\frac{(\mathbf{k}|\mathbf{p}\cdot\mathbf{e}_s|b\mathbf{k})(b\mathbf{k}|\mathbf{p}\cdot\mathbf{e}_i|\mathbf{k})}{\varepsilon_\mathbf{k}-\varepsilon_{b\mathbf{k}}+\omega_i}+\frac{(\mathbf{k}|\mathbf{p}\cdot\mathbf{e}_i|b\mathbf{k})(b\mathbf{k}|\mathbf{p}\cdot\mathbf{e}_s|\mathbf{k})}{\varepsilon_\mathbf{k}-\varepsilon_{b\mathbf{k}}-\omega_s}\right] \tag{2.2}$$

where m is the electron mass and b stands for the band index of the electron excited out of the conduction band, and the corresponding states are $|\mathbf{k}b\rangle$ and $|\mathbf{k}\rangle$, respectively. In the case of time-reversal symmetry,

$$\gamma_\mathbf{k}=\gamma_{-\mathbf{k}^*} \tag{2.3}$$

holds. $\gamma_\mathbf{k}$ does not depend on $\mathbf{q}$, as $q\ll k_F$, but it is very sensitive to the polarization directions of the light.

The scattering probability is determined by the susceptibility

$$\chi_{\tilde{\rho}\tilde{\rho}}(\mathbf{q},\tau-\tau')=-\langle T_\tau[\tilde{\rho}_\mathbf{q}(\tau)\tilde{\rho}_{-\mathbf{q}}(\tau')]\rangle\ , \tag{2.4}$$

where $\langle\ \rangle$ denotes the thermal average and T_τ is the complex time τ ordering operator. Its Fourier transformation is

$$\chi_{\tilde{\rho}\tilde{\rho}}(\mathbf{q},\omega_n)=\tfrac{1}{2}\int_{-T}^{T}d(\tau-\tau')e^{i\omega_n(\tau-\tau')}\chi_{\tilde{\rho}\tilde{\rho}}(\mathbf{q},\tau-\tau')\ , \tag{2.5}$$

where T is the temperature and $\omega_n=2\pi nT$, where n is an integer.

The cross section is proportional to the generalized dynamical structure factor $\tilde{S}(\mathbf{q},\omega)$, which is expressed by the analytical continuation of $\chi_{\tilde{\rho}\tilde{\rho}}(\mathbf{q},\omega_n)$ as

$$\tilde{S}(\mathbf{q},\omega)=[1+n_B(\omega)]\left[-\frac{1}{\pi}\mathrm{Im}\chi_{\tilde{\rho}\tilde{\rho}}(\mathbf{q},z=\omega+i\delta)\right]\ , \tag{2.6}$$

where n_B is the Bose distribution and $\delta\to0$.

B. Long-range Coulomb effects

In the case where the light produces charge fluctuation in the electron gas, the coupling to the long-range Coulomb forces reduces the scattering rate. Therefore, it is useful to treat these forces separately. The relevant diagrams are shown in Fig. 2. Coulomb lines for which the diagram splits by their removal must be treated separately. Considering only the diagrams without such Coulomb lines, the following polarization terms are defined:

$$\pi_{\gamma\gamma}(\mathbf{q},\tau-\tau')=-\langle T_\tau[\tilde{\rho}_\mathbf{q}(\tau)\tilde{\rho}_{-\mathbf{q}}(\tau')]\rangle\ , \tag{2.7a}$$

$$\pi_{\gamma0}(\mathbf{q},\tau-\tau')=-\langle T_\tau[\tilde{\rho}_\mathbf{q}(\tau)\rho_{-\mathbf{q}}(\tau')]\rangle\ , \tag{2.7b}$$

$$\pi_{0\gamma}(\mathbf{q},\tau-\tau')=-\langle T_\tau[\rho_\mathbf{q}(\tau)\tilde{\rho}_{-\mathbf{q}}(\tau')]\rangle\ , \tag{2.7c}$$

$$\pi_{00}(\mathbf{q},\tau-\tau')=-\langle T_\tau[\rho_\mathbf{q}(\tau)\rho_{-\mathbf{q}}(\tau')]\rangle\ , \tag{2.7d}$$

where the charge operator $\rho_\mathbf{q}$ is defined Eq. (2.1) with $\gamma=1$. The Coulomb energy operator is

$$H_c=\tfrac{1}{2}\sum_q\rho_\mathbf{q}\frac{4\pi e^2}{q^2}\rho_{-\mathbf{q}}\ . \tag{2.8}$$

The summation of the diagrams in Fig. 2 gives the total susceptibility $\chi_{\tilde{\rho}\tilde{\rho}}(\mathbf{q},\omega)$

$$\chi_{\tilde{\rho}\tilde{\rho}}=\pi_{\gamma\gamma}+\pi_{\gamma0}\left[\frac{4\pi e^2}{q^2}+\frac{4\pi e^2}{q^2}\pi_{00}\frac{4\pi e^2}{q^2}+\cdots\right]\pi_{0\gamma}\ , \tag{2.9}$$

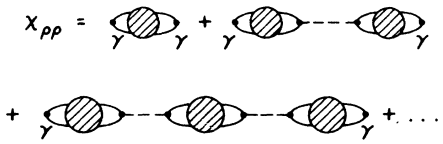

FIG. 2. The diagrams contributing to the generalized density-density correlation function $\chi\tilde{\rho}\tilde{\rho}$ are depicted [see Eq. (2.9)]. The Coulomb interaction with small momentum transfer is represented by dashed line. The circles represent the free particle propagations and the vertex corrections due to the interaction between the particles except those depicted by the dashed lines; thus the circles contain the vertical Coulomb lines also. The dots correspond to the density operators and the effective density $\tilde{\rho}$ is labeled by γ.

which can be rewritten as

$$\chi_{\tilde{\rho}\tilde{\rho}}=\left[\pi_{\gamma\gamma}-\frac{\pi_{\gamma 0}\pi_{0\gamma}}{\pi_{00}}\right]+\frac{\pi_{\gamma 0}\pi_{0\gamma}}{\pi_{00}^2}\chi_{\rho\rho}\ , \tag{2.10}$$

where

$$\chi_{\rho\rho}=\pi_{00}\Big/\left[1-\frac{4\pi e^2}{q^2}\pi_{00}\right] \tag{2.11}$$

is the density-density response function, which in the $\mathbf{q}\to 0$ limit behaves like $\chi\sim(v_F q)^2/\omega_p^2$, where ω_p is the plasma frequency. This behavior persists even in the superconducting state as will be shown in Sec. IV B 1. Thus, for small $\mathbf{q}$ only the term in the bracket is important on the right-hand side of Eq. (2.10). A similar argument was used by Abrikosov and Genkin[25] and by Klein and Dierker.[21]

C. Hamiltonian and scattering channels

One conduction band is considered with energy $\varepsilon_{\mathbf{k}}$, and the dispersion is linearized at the Fermi energy; thus the terms proportional to the effective mass are neglected as they result only in smaller corrections. Thus the unperturbed Hamiltonian with energy $\varepsilon_{\mathbf{k}}$ measured from the Fermi energy is

$$H_0=\sum_{\mathbf{k},\sigma}\varepsilon_{\mathbf{k}}a^{\dagger}_{\mathbf{k},\sigma}a_{\mathbf{k},\sigma}\ . \tag{2.12}$$

The general electron-electron interaction is given by the Hamiltonian

$$H_1=\frac{1}{2V}\sum_{\substack{\mathbf{k}_1+\mathbf{k}_2=\mathbf{k}_3+\mathbf{k}_4\\ \sigma,\sigma'}}a^{\dagger}_{\mathbf{k}_1,\sigma}a^{\dagger}_{\mathbf{k}_2,\sigma'}(\mathbf{k}_1,\sigma;\mathbf{k}_2,\sigma'|V|\mathbf{k}_3,\sigma';\mathbf{k}_4,\sigma)a_{\mathbf{k}_3,\sigma'}a_{\mathbf{k}_4,\sigma}\ , \tag{2.13}$$

which is determined by the matrix element $(|V|)$. This Hamiltonian acts in the two-particle (Cooper) and the electron-hole (zero-sound) channels, shown in Fig. 3.

In general, the polarization dependence of the Raman scattering strength $\gamma_{\mathbf{k}}$, the interaction matrix element $(|V|)$, the electron dispersion $\varepsilon_{\mathbf{k}}$ as well as the momentum-dependent superconducting gap $\Delta_{\mathbf{k}}$ can break the rotational symmetry even for a spherical or cylindrical Fermi surface. In the general case these functions can be expanded in terms of crystal harmonics. The generalization is straightforward, thus we assume that only the Raman strength $\gamma_{\mathbf{k}}$ breaks the symmetry that can be expanded in terms of spherical harmonics $Y_{lm}(\theta,\phi)$ or Fourier terms $e^{im\phi}$ depending on the dimensionality $(d=3,2)$, where the angles (θ,ϕ) determine the direction of the momentum. In general

$$\gamma_{\mathbf{k}}=\sum_L\gamma_L\phi_L(\mathbf{k})\ , \tag{2.14}$$

where ϕ_L forms a complete set of functions. As the total momenta of the particles both in the Cooper or zero-sound channels are very small; therefore $(|V|)$ depends only on two momenta. Considering the channels separately, as shown in Fig. 3(a), 3(b), and 3(c), in the Cooper channel

$$(\mathbf{k},\sigma;-\mathbf{k},-\sigma|V|-\mathbf{k}',-\sigma;\mathbf{k}',\sigma)=-\sum_{L,L'}\phi_L(\mathbf{k})g^C_{LL'}\phi_{L'}(\mathbf{k}')^* \tag{2.15}$$

and in the zero-sound channel

$$(\mathbf{k}',\sigma;\mathbf{k},\sigma|V|\mathbf{k}',\sigma;\mathbf{k},\sigma)=\sum_{L,L'}\phi_L(\mathbf{k})g^Z_{LL'}\phi_{L'}(\mathbf{k}')^* \tag{2.16}$$

for $L,L'\neq 0$ and

$$(\mathbf{k}',-\sigma;\mathbf{k},\sigma|V|\mathbf{k},\sigma;\mathbf{k}',-\sigma)=-\phi_0(\mathbf{k})g^Z_0\phi_0(\mathbf{k}') \tag{2.17}$$

for $L=0$, where $\phi_{L=0}$ is a constant. The simplification in the last equation (2.17) holds for most of the interactions. The different signs on the right-hand side of Eqs. (2.16) and (2.17) are associated with the different order of operators and are introduced for further convenience. Furthermore, in Eq. (2.16) $L,L'\neq 0$.

If the interaction is rotation invariant, then $g^Z_{LL'}=\delta_{LL'}g^Z_L$ and $g^C_{LL'}=\delta_{LL'}g^C_L$ are diagonal in spherical harmonics basis. The more general case is discussed by Klein and Dierker.[21] Assuming the BCS interaction with strength g^* the following identities hold:

$$g^C_0=g^Z_0=g^* \tag{2.18}$$

for the channel $L=0$. Additionally, the residual interac-

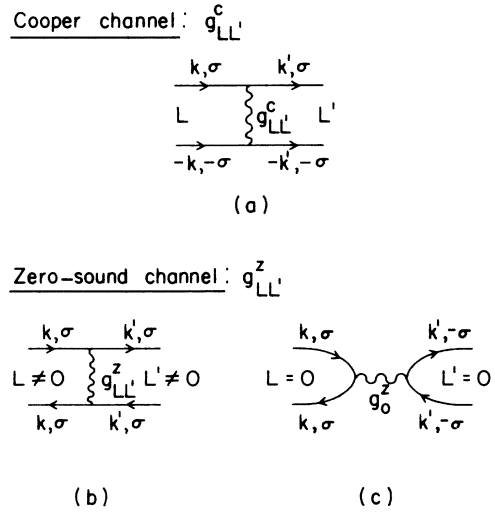

FIG. 3. The interactions introduced by Eqs. (2.15)–(2.17) are represented by wavy lines in the Cooper (C) and the zero-sound (Z) channels. In these channels the states characterized by L and L' quantum numbers are connected by the interaction.

tions in channels $L\neq 0$ are introduced for which

$$g_L^C=-g_L^Z=g_L \quad (L\neq 0) \tag{2.19}$$

holds. For attractive interaction $g^*>0$ and $g_L>0$ and for BCS ground state $g^*>g_L$, but g_L is not necessarily attractive.

In order to describe the superconductivity we use the Gor'kov formulation. The Fourier transform of the normal Green's function $G_{\alpha\beta}(x,x')=\delta_{\alpha\beta}G(x-x')$ is

$$G(\mathbf{k},\omega_n)=-\frac{i\omega_n+\varepsilon_{\mathbf{k}}}{\omega_n^2+\varepsilon_{\mathbf{k}}^2+\Delta^2}\ , \tag{2.20}$$

while the anomalous Green's functions are defined as

$$F_{\alpha\beta}(xx')=\langle T_\tau[\psi_\alpha(x)\psi_\beta(x')]\rangle=-I_{\alpha\beta}F(x-x')\ , \tag{2.21}$$

$$F^\dagger_{\alpha\beta}(xx')=\langle T_\tau[\psi^\dagger_\alpha(x)\psi^\dagger_\beta(x')]\rangle=I_{\alpha\beta}F(x-x')\ , \tag{2.22}$$

where $x=(\mathbf{x},\tau)$ is the four-component coordinate, ψ is the electron field operator, the spin matrix I is

$$I=\begin{bmatrix}0 & 1\\ -1 & 0\end{bmatrix} \tag{2.23}$$

and

$$F(\mathbf{k},\omega_n)=\frac{\Delta}{\omega_n^2+\varepsilon_{\mathbf{k}}^2+\Delta^2} \tag{2.24}$$

is the Fourier transform of $F(x-x')$. Finally the gap equation for zero temperatures is

$$1=\tfrac{1}{2}g^*\rho_0\int_{-\omega_D}^{\omega_D}\frac{d\varepsilon}{(\Delta^2+\varepsilon^2)^{1/2}}\ , \tag{2.25}$$

where ω_D is the energy cutoff and ρ_0 is the density of the electron states at the Fermi surface for one spin direction ($\rho_0=k_Fm/2\pi^2$ for spherical and $\rho_0=k_Fm/4\pi c$, for cylindrical Fermi surface with size πc in the axial direction).

III. VERTEX EQUATIONS AND THE SOLUTION

In the following the main task is to calculate the polarization functions defined by Eqs. (2.7a)–(2.7d). These polarization functions correspond to the diagrams in Fig. 4

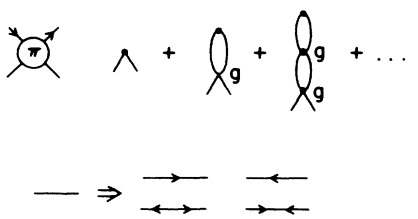

FIG. 4. The corrections to the density vertex are depicted. The solid line represents the electrons. Each line must be decorated by a single or two arrows shown in the lower part of the figure where the first row corresponds to the normal and the second one to the anomalous Green's functions. Only those diagrams must be considered where the charge is conserved at each vertex. The interaction points are labeled by g.

where the diagrams start with an electron-hole pair that propagates with normal and anomalous Green's function, and they interact with each other. The starting bare vertex may contain a weight function $\phi_L(\mathbf{k})$ depending on which polarization term is calculated. Including the effect of residual interaction the following quantities can be introduced:

$$\pi^{\mu\nu}_{LL'}(\mathbf{q};\tau-\tau')=-\langle T_\tau[Q^\mu_L(q,\tau)Q^\nu_{L'*}(-\mathbf{q},\tau')]\rangle\ , \tag{3.1}$$

where $\mu,\nu=0,+,-$ and L'^* stands for $\phi^*_{L'}(\mathbf{k})$ in the following quantities:

$$Q^0_L(\mathbf{q},\tau)=\frac{1}{\sqrt{2}V}\sum_{\mathbf{k},\alpha}\phi_L(\mathbf{k})a^\dagger_{\mathbf{k}+\mathbf{q},\alpha}(\tau)a_{\mathbf{k},\alpha}(\tau)\ , \tag{3.2}$$

$$Q^+_L(\mathbf{q},\tau)=\frac{1}{V}\sum_{\mathbf{k},\alpha}\alpha\phi_L(\mathbf{k})a^\dagger_{\mathbf{k}+\mathbf{q},\alpha}(\tau)a^\dagger_{-\mathbf{k},-\alpha}(\tau)\ , \tag{3.3}$$

$$Q^-_L(\mathbf{q},\tau)=-\frac{1}{V}\sum_{\mathbf{k},\alpha}\alpha\phi_L(\mathbf{k})a^+_{-\mathbf{k}-\mathbf{q},-\alpha}(\tau)a^+_{\mathbf{k},\alpha}(\tau)\ . \tag{3.4}$$

Similar quantities defined with the BCS Green's function but without the residual interaction are labeled by (0) as

$$\pi^{\mu\nu(0)}_{LL'}(\mathbf{q};\tau-\tau')\ .$$

In order to sum up the diagrams shown in Fig. 4, the following matrix vertex equation must be solved to obtain $\pi^{\mu\nu}_{LL'}(\mathbf{q},\omega_n)$:

$$\hat{\pi}=\hat{\pi}^{(0)}+\hat{\pi}\hat{\hat{g}}\hat{\hat{\pi}}^{(0)}\ , \tag{3.5}$$

where

$$\hat{\pi}=(\pi^{00},\pi^{0+},\pi^{0-}) \tag{3.6}$$

and similarly holds for $\hat{\pi}^{(0)}$; furthermore

$$\hat{\hat{\pi}}^{(0)}=\begin{bmatrix}\pi^{00(0)} & \pi^{0+(0)} & \pi^{0-(0)}\\ \pi^{+0(0)} & \pi^{++(0)} & \pi^{+-(0)}\\ \pi^{-0(0)} & \pi^{-+(0)} & \pi^{--(0)}\end{bmatrix}\ , \tag{3.7}$$

and, finally, the coupling matrix is

$$\hat{\hat{g}}^{(0)}=\begin{bmatrix}-g^Z & 0 & 0\\ 0 & 0 & g^C\\ 0 & g^C & 0\end{bmatrix}\ . \tag{3.8}$$

We assume the following: (i) The superconductivity is BCS type and the gap is isotropic. (ii) The Fermi surface is a sphere or cylinder. (iii) The one-particle band energy $\varepsilon_{\mathbf{k}}$ is isotropic. (iv) The residual interactions in channels $L\neq 0$ are rotationally invariant, and Eq. (3.5) is diagonal in the channel indexes for $L=0$ and $L\neq 0$ as well. In each separate channel the diagonal matrix elements of the couplings defined by Eqs. (2.15)–(2.17) must be used. The derivation of Eqs. (3.5)–(3.8) is lengthy but straightforward.

In the more general case these equations have matrix structure in the channel indexes and their solution is more complicated. For further discussion see Sec. III.5 in Ref. 21.

The $\hat{\hat{\pi}}$ matrix can be given in terms of the Green's function in coordinate representation as

$$\hat{\bar{\pi}}(x-x')=\begin{bmatrix} G\bar{G}-F^2 & \sqrt{2}FG & -\sqrt{2}F\bar{G} \\ \sqrt{2}F\bar{G} & F^2 & \bar{G}^2 \\ -\sqrt{2}FG & G^2 & F^2 \end{bmatrix}, \tag{3.9}$$

where $G=G(x-x')$, $\bar{G}=G(x'-x)$, and $F=F(x-x')$. This result holds for each channel independently for isotropic superconductors.

The Fourier transforms of the matrix elements can be calculated directly using Eqs. (2.20) and (2.24); only one ω_n summation must be performed. The matrix structure of the result is

$$\hat{\bar{\pi}}^{(0)}(\mathbf{q};\omega_n)=\begin{bmatrix} A & C & C \\ -C & B & D \\ -C & D & B \end{bmatrix}. \tag{3.10}$$

In general the functions A, B, C, and D are defined by Eq. (3.9) and for zero temperature their expressions are given in Appendix A in integral forms. Their limits at $q=0$ and the first expansion terms are presented in Appendixes B and C.

After applying a unitary transformation

$$\hat{\bar{U}}=\begin{bmatrix} 1 & 0 & 0 \\ 0 & 1/\sqrt{2} & 1/\sqrt{2} \\ 0 & -1/\sqrt{2} & 1/\sqrt{2} \end{bmatrix}, \tag{3.11}$$

the solution of the vertex Eq. (3.5) can be given a simple form introducing the unit matrix

$$\hat{\bar{\pi}}\,\hat{\bar{U}}=\hat{\bar{\pi}}^{(0)}\,\hat{\bar{U}}(\hat{\bar{I}}-\hat{\bar{U}}^{-1}\hat{\bar{g}}\,\hat{\bar{\pi}}^{(0)}\,\hat{\bar{U}})^{-1}, \tag{3.12}$$

which split to a 2×2 and 1×1 matrix after using Eq. (3.10). This splitting corresponds to the separation of the amplitude and phase modes, but as can be seen from the algebra, only the amplitude mode is coupled to the light (the third component of the vector $\hat{\bar{\pi}}^{(0)}\,\hat{\bar{U}}$ vanishes).

The final result for $\pi^{00}(\mathbf{q};\omega_n)$ has the form

$$\pi^{00}=\frac{A-g^C A(D+B)-2g^C C^2}{1+g^Z A-g^C(D+B)-g^Z g^C A(D+B)-2g^Z g^C C^2}, \tag{3.13}$$

which also holds for each channel independently. The intensity of the Raman scattering can be obtained by inserting Eqs. (3.13), (2.14), and (2.10) into (2.6). The remaining task is to use the explicit expressions of A, B, C, and D, given in Appendixes B and C.

IV. PHYSICAL RESULTS

A. q=0 limit and bound states ($L\neq0$)

Considering an $L\neq0$ channel that does not couple to the Coulomb field, only the first term on the right-hand side of Eq. (2.10) contributes; thus the Raman scattering is proportional to

$$|\gamma_L|^2\mathrm{Im}\pi^{00}_{LL}(\mathbf{q};\omega_n)|_{i\omega_n\to\omega+i\delta}\,.$$

As we have discussed in the Introduction, bound states are formed and the continuum is renormalized. To obtain these results expressions (B2)–(B5) for the A, B, C, and D coefficients must be inserted into Eq. (3.13) for π^{00} and the analytical continuation to the real axis must be taken

$$[\pi^{00}_{LL}(\mathbf{q},\omega_n)\to\pi^{00}_{LL}(\mathbf{q},\omega)]\,.$$

The result can be expressed by the function

$$I_0(z)=\int_{-\infty}^{\infty} dx\,\frac{1}{z+x^2}\,\frac{1}{(x^2+1)^{1/2}}, \tag{4.1}$$

where $z=1-\omega^2/4\Delta-i\delta$, and $\delta\to+0$. The analytical expressions for different regions are given by Eqs. (B6a)–(B6c) in Appendix B.

The general result obtained is

$$\mathrm{Im}\pi^{00}(\mathbf{q}=0;\omega)=\tfrac{1}{2}\rho_0\frac{\mathrm{Im}I_0\left[1-\frac{\omega^2}{4\Delta^2}\right]}{\left[1-\alpha_L\left[\frac{\omega}{2\Delta}\right]\mathrm{Re}I_0\left[1-\frac{\omega^2}{4\Delta^2}\right]\right]^2+\left[\alpha_L\left[\frac{\omega}{2\Delta}\right]\mathrm{Im}I_0\left[1-\frac{\omega^2}{4\Delta^2}\right]\right]^2}, \tag{4.2}$$

where $\alpha_L(\omega/2\Delta)$ is a slowly varying function of the energy and plays the role of a dimensionless coupling constant

$$\alpha_L(\omega/2\Delta)=\frac{1}{2}\left[\rho_0 g_L^Z+\frac{\omega^2}{4\Delta^2}\frac{\rho_0 g_L^C}{1-g_L^C/g^*}\right], \tag{4.3}$$

where g^* appears as one of the integrals, expressed with the help of the BCS gap Eq. (2.25). In the special case where Eq. (2.19) $g_L^C=-g_L^Z=g_L$ holds, for the couplings near the gap edge, $\omega=2\Delta$ has a simple form

$$\alpha_L=\tfrac{1}{2}\rho_0 g_L\frac{g_L/g^*}{1-g_L/g^*}. \tag{4.4}$$

As the ground state is formed by Cooper pairs, $g_L<g^*$ must hold. In general, the parameter α can, however, take, arbitrary values ($-\infty<\alpha<\infty$). It can be very small, e.g., $\alpha=5\times10^{-3}$ for $\rho_0 g^*=0.2$ and $g_L=0.2g^*$. A typical value may be $\alpha=0.05$–0.1 with $\rho_0 g^*=0.2$ and $g_L=0.5g^*$.

The formula given by Eq. (4.2) was first derived for Ra-

man scattering in superconductors by Klein and Dierker.[21] A very similar expression was derived by Ruvalds and Zawadowski[15,17] for Raman scattering on roton pairs in liquid ^{4}He in which case α is the roton-roton scattering strength in the angular momentum channel $l=2$. However, the first term of the denominator was derived much earlier by Bardasis and Schrieffer,[6] in studying bound states in the gap region.

1. *Bound states* ($L\neq 0$)

Bound states form when the denominator of the expression (4.2) vanishes at the energy of the bound state $\omega=\omega_L$; thus $\mathrm{Im}I_0=0$ for $\omega<2\Delta$ [see Eqs. (B6a)–(B6c)] and

$$1-\alpha_L\left[\frac{\omega_L}{2\Delta}\right]\mathrm{Re}I_0\left[1-\frac{\omega^2}{4\Delta^2}\right]=0\ . \tag{4.5}$$

As $\mathrm{Re}I_0>0$, for $\omega<2\Delta$ [see Eq. (4.1) or Eq. (B6a)], α must be positive to obtain a bound state. Using the relation given by Eq. (2.19) $g_L^C=-g_L^Z=g_L$, it turns out that $\alpha>0$ holds for arbitrary sign of g_L. The expression (4.3) contains two terms, the first one arises from the electron-hole channel (Z) and the second from the two-electron channel (C). For attractive interaction ($g_L<0$) the second term dominates, while for a repulsive one ($g_L<0$) the first applies.

That interesting result is interpreted by Bardasis and Schrieffer,[6] as in the first case an electron pair is formed that is orthogonal to the Cooper pair ($L\neq 0$), while in the second case an exciton is formed. In the Anderson-Rickayzen[2] approximation the zero-sound channel is ignored, thus no exciton-like excitation has been found. Furthermore, ω_L cannot be negative for $g_L<0$, because then an excitonic insulator is formed instead of a superconductor. This feature is in contrast to the two-roton bound state in liquid ^{4}He, where the sign of the roton-roton interaction can be arbitrary and can be changed by pressure.[27,28]

The strength of the bound-state pole can be obtained by linearizing the denominator of Eq. (4.2) around the bound state and its strength Z_L [$\mathrm{Im}\pi_{LL}^{00}\sim Z_L\delta(\omega-\omega_L)$ for $\omega<2\Delta$] is given by

$$Z_L=\tfrac{1}{2}\rho_0\pi\left\{\frac{\partial}{\partial\omega}\left[\alpha_L(\omega)\mathrm{Re}I_0\left[1-\frac{\omega^2}{4\Delta^2}\right]\right]\right\}^{-1}_{\omega=\omega_L}\ . \tag{4.6}$$

The binding energies are plotted in Figs. 6 and 7 of Ref. 6 both for positive and negative g_L. For a small binding energy $\omega_{B,L}=2\Delta-\omega_L$ ($\omega_L\sim 2\Delta$), the simplified expression of α given by Eq. (4.4) can be used. The equations of Sec. III A of Ref. 17 provide detailed information after replacing the roton-roton coupling g_4 by α and the energy scale D by 2Δ. For small couplings $0<\alpha\ll 1$, $\omega_{B,L}\sim\Delta\alpha_L^2$, and $Z_L\sim\rho_0\alpha_L^2$. Furthermore, if $g_L\to g^*$ then $\omega_L\to 0$.

2. *Continuum* ($L=0$)

The formula (4.2) describes the continuum formed above the threshold ($\omega>2\Delta$). Without the final-state interaction ($\alpha_L\equiv 0$), the spectrum exhibits a square-root singularity like $(\omega^2-4\Delta^2)^{-1}$ at $\omega=2\Delta$ with strength in the Raman spectrum proportional to γ_L^2 (see Fig. 1). The residual interaction deforms the spectrum in such a way that above the threshold a maximum is formed in the continuum. The stronger the coupling is [$\alpha_L(\omega/2\Delta\sim 1)$], the larger the shift of the maximum is from the threshold. At the threshold $\omega=2\Delta$ the spectrum vanishes as the imaginary part of the function I_0 has square-root singularity [see Eq. (B6c)].

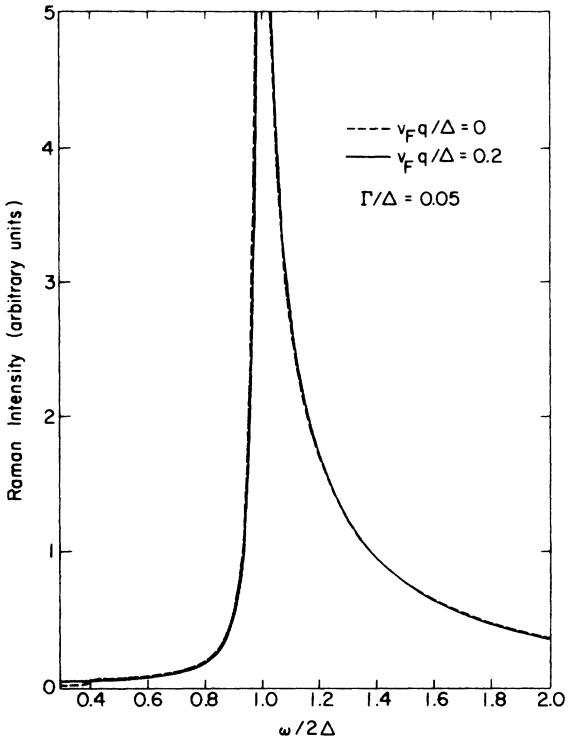

FIG. 5. The Raman intensity calculated with Eq. (3.13) for finite value of $v_F q/\Delta=0.2$ (solid line) and $v_F q/\Delta=0$ (dashed line) is shown. The line broadening $\Gamma/\Delta=0.05$ and a coupling strength of $\alpha=0.025$ are used.

For weak coupling, the total spectrum is very similar to the one shown in Fig. 1(b). If the bound state is convoluted with a Lorentzian distribution characterizing the experimental resolution Γ_{exp} it is clear that a smeared curve may exhibit a single maximum [see Figs. 1(b) and 5]. The position of the maximum is different for the different channels as the couplings α_L are different. As the polarization of the incident and scattered light determines the strength γ_L^2 of the channel L in the spectrum, thus the peak in the spectrum is expected to be shifted by changing the polarization. In anisotropic superconductors the anisotropy of the gap must result in additional shifts.

B. Small q extension

1. *General remarks*

By transferring momentum $\mathbf{q}$ to the material, a Cooper pair can be broken into two excitations with momenta

$\mathbf{k}+\mathbf{q}/2$ and $\mathbf{k}-\mathbf{q}/2$, where $\mathbf{k}$ is an arbitrary vector. As the energy of a single excitation is $E_{\mathbf{k}}=(\Delta^2+\varepsilon_{\mathbf{k}}^2)^{1/2}$, therefore for a fixed angle θ between $\mathbf{q}$ and $\mathbf{k}$ the continuum has a lower threshold that depends on that angle. Thus, considering the energy integral with respect to ξ, which replaces the momentum integral perpendicular to the Fermi surface, the poles in the loop expansion for A, B, C, and D, given in Appendix A, vary on the Fermi surface [see Eqs. (A4)–(A7)].

The denominators of the expressions (A4)–(A7) after analytical continuation $i\omega_n \rightarrow \omega + i\delta$ can be factorized as

$$(E_{\mathbf{k}+\mathbf{q}/2}+E_{\mathbf{k}-\mathbf{q}/2})^2-\omega^2=\frac{4}{E^2}\left[\Delta^2+\xi^2-\frac{(\mathbf{v}_F\mathbf{q})^2}{\omega^2}\Delta^2\right] \times\left[\Delta^2+\xi^2-\frac{\omega^2}{4}+\frac{(\mathbf{v}_F\mathbf{q})^2}{\omega^2}\Delta^2\right], \tag{4.7}$$

where $\varepsilon_{\mathbf{k}}=\xi$ and $E^2=\Delta^2+\xi^2$. In Appendix C partial fraction decomposition is used. Furthermore, it is assumed that for the relevant momentum transfer $\mathbf{q}$

$$\frac{|\mathbf{q}\cdot\mathbf{v}_F|}{\Delta}\ll 1 \tag{4.8}$$

holds as $q\sim\delta^{-1}$ where the penetration depth of the light $\delta<200$ Å. The other form of this assumption is that $\delta/\xi_0\gg 1$, where ξ_0 is the BCS coherence length.

There are three characteristic energy regions:

region I: $v_F q \ll \omega < 2\Delta$,

region II: $2\Delta<\omega<2\Delta\left[1+\frac{(qv_F)^2}{\omega^2}\right]^{1/2}$,

region III: $2\Delta\left[1+\frac{(qv_F)^2}{\omega^2}\right]^{1/2}<\omega$.

For normal superconductors where the gap is small and $\delta/\xi_0\lesssim 1$, region II dominates. In A-15, heavy fermion, high-T_c materials $\delta/\xi_0\gg 1$; therefore $(\mathbf{q}\cdot\mathbf{v}_F)/\Delta$ serves as a small expansion parameter, as has been discussed by Abrikosov and Fal'kovskii,[24] and also by Klein and Dierker.[21] The first authors studied two extreme limits and an intermediate region: (i) the lower edge of region II, (ii) the intermediate region $\omega\sim(\omega^2-\Delta^2)^{1/2}$ where the behavior is already smooth, and (iii) the high-energy side of region III, where the behavior is like that in a normal metal ($\sim\omega^{-2}$). These regions, however, do not cover the region where the strong changes and the maximum have been found. They showed that at the low-energy edge of region II the Raman spectrum goes to zero like $q^3\ln^{-2}(\omega^2-4\Delta^2)$ as $\omega\rightarrow 2\Delta$ [see Eqs. (19) and (22a) in Ref. 24]. Klein and Dierker[21] studied regions I and III by taking the $q\rightarrow 0$ limit.

In what follows, region II will be ignored as it is so narrow that it does not contribute essentially to a spectrum with finite experimental resolution. Thus in region II the results obtained from region III are continued in a way that the spectrum goes smoothly to zero as $\omega\rightarrow 2\Delta$.

In Appendix C the polarization functions $\pi(\mathbf{q};\omega)$ are calculated for arbitrary ω in order to demonstrate the anomalous q behavior at the lower edge of region II [case (i) in Abrikosov and Fal'kovskii's calculation (Ref. 24)] and to show that these anomalies are absent in region III.

2. *Plasma oscillation* ($L=0$)

The plasma oscillations are the consequence of the long-range Coulomb forces that occur in the zero-sound channel. The Coulomb force can be added to the coupling g_0^Z introduced by Eq. (2.17). As the short-range force acts only between two electrons with opposite spins and, on the other hand, there is no restriction on the spin in the Coulomb interaction, therefore the strength of the Coulomb field must be multiplied by 2, thus the replacement

$$g_0^Z\rightarrow g_0^Z+\frac{8\pi e^2}{q^2} \tag{4.9}$$

must be carried out and $g_0^Z=g_0^C=g^*$ holds [see Eq. (2.18)].

In order to get the response function π^{00} in channel $L=0$ the small q expansions for the quantities A, B, C, and D [given by Eqs. (C10)–(C13)] must be inserted in Eq. (3.13).

Because of Eq. (2.18), such a combination of the A, B, C, and D coefficient occurs in the numerator of π^{00}, which disappears in the $q\rightarrow 0$ limit [see Eq. (B2)–(B5)]. Thus, one can write

$$A(q,\omega)-g^*A(q,\omega)[B(q,\omega)+D(q,\omega)]-2g^*C^2(q,\omega)=\frac{(qv_F)^2}{\Delta^2}\rho_0\chi(q,\omega) , \tag{4.10}$$

where $\lim_{q\rightarrow 0}\chi(q,\omega)=\chi(\omega)$ can be directly determined from Eqs. (C10)–(C13).

Using this notation and Eq. (B1) one gets for small q that

$$\pi^{00}(q;\omega)=\frac{\left[\frac{qv_F}{\Delta}\right]^2\rho_0\chi(\omega)}{1-g^*[B(\omega)+D(\omega)]_{q=0}-\frac{8\pi e^2}{\Delta^2}v_F^2\rho_0\chi(\omega)} . \tag{4.11}$$

From Eqs. (B1), (B3), and (B5)

$$1-g^*[B_0(\omega)+D_0(\omega)]=-\tfrac{1}{8}g^*\rho_0\frac{\omega^2}{\Delta^2}I_0\left[1-\frac{\omega^2}{4\Delta^2}\right] . \tag{4.12}$$

Introducing the plasma frequency ω_p for a spherical Fermi surface

$$\omega_p^2=\frac{8\pi}{3}e^2v_F^2\rho_0 \tag{4.13}$$

the last term in the denominator of Eq. (4.11) can be written as $3\omega_p^2\chi(\omega)/\Delta^2$. It is easy to show that for smaller

energies $2\Delta < \omega \ll \omega_p$ the ratio of these two terms has the order of ω_p^2/Δ^2, thus there are no zeros for the denominator and as $\omega \to 2\Delta$, that ratio becomes even larger.

The plasma pole occurs at $\omega = \omega_p$, thus asymptotic formulas valid for $\omega/\Delta \gg 1$ must be used. The asymptotic expression for χ can be obtained by a lengthy but straightforward calculation based on Appendix C and the result is

$$\chi(\omega) \sim -g^* \frac{1}{24} \frac{1}{\Delta^2} I_0 \left[1 - \frac{\omega^2}{4\Delta^2} \right], \tag{4.14}$$

where the identity $S_0^{-1} \int dS (\mathbf{v}_F \cdot \mathbf{q})^2 = (v_F q)^2/3$ is also used.

3. *Continuum in channel $L = 0$*

The continuum can be obtained by taking the imaginary part of Eq. (4.11). It has already been mentioned that the term proportional to χ dominates the denominator, thus

$$\mathrm{Im}\pi^{00}(q;\omega) = \frac{(qv_F)^2}{\Delta^2} \rho_0 g^* \frac{\mathrm{Im}\{[B_0(\omega) + D_0(\omega)]\chi(\omega)\}}{[3(\omega_p^2/\Delta^2)]^2 |\chi(\omega)|^2}$$

$$\sim \frac{(qv_F)^2}{\Delta^2} \frac{\Delta^2}{\omega_p^2} \ll 1 \tag{4.15}$$

therefore the contribution of channel $L = 0$ is negligibly small. It can be shown again that at the threshold $\omega = 2\Delta$ the spectrum disappears as $\mathrm{Im}I_0(z)$ is the only diverging function.

4. *Continuum in channels $L \neq 0$*

In Sec. IV B 2 the continuum in the $q = 0$ limit has already been calculated with couplings given by Eq. (2.19). The first correction can be obtained on the basis of Eq. (3.13) using the expressions (C9)–(C13). In expression (C9) there is one integral over the Fermi surface to be performed. The integrand is a product of the factor $(\mathbf{v}_F \cdot \mathbf{q})^2$ and one of the functions A_2, B_2, C_2, and D_2. The latter ones also depend on q as their argument, z is sensitive on q. Thus the integral either must be carried out numerically or the assumption $\omega^2 - (2\Delta)^2 \gg (v_F q)^2$ must be made. In the second case the arguments z and z' of the functions I_n can be replaced by their value with $q = 0$, as I_n $(n = 0,1,2)$ are slowly varying functions everywhere except at $\omega \sim 2\Delta$. The results for both $q = 0$ and finite q are shown on Fig. 5. The calculated spectra demonstrate that the Raman spectrum is not sensitive on the momentum transfer q as far as $(v_F q)^2 \ll (2\Delta)^2$ holds, even for $v_F q$ as large as 0.2Δ. Finally, it must be mentioned that this calculation is valid only in region III not very near the boundary line between regions II and III. Since region II is very narrow in the limit $(v_F q)^2 \ll (2\Delta)^2$, we calculate the curve in Fig. 5 by extrapolating from region III to $\omega = 2\Delta$.

V. SUMMARY

The theory of Raman scattering in a single band BCS superconductor has been developed. For the A-15 compounds and the high-T_c superconductors $v_F q/\Delta$ is a small parameter. It is found that the Klein-Dierker theory[21] established in the $q \to 0$ limit is correct in that limit. On the other hand, the Abrikosov-Fal'kovskii theory[24] deals with the first nonvanishing correction to that; however, it is limited to a very small energy region near the threshold

$$2\Delta < \omega < 2\Delta \left[1 + \left(\frac{v_F q}{\Delta} \right)^2 \right]^{1/2}$$

or to rather high energies. That former region is almost negligible for the high-T_c materials but may be relevant in cases where $v_F q/\Delta$ is not very small but still smaller than unity. This theory covers the complete energy region provided that the momentum transfer is small.

For the sake of simplicity, this theory is completely rotationally invariant; the Fermi surface is a sphere or a cylinder, depending on the effective dimensionality of the material. In that case the different angular momentum scattering channels characterized by $L = (l,m)$ or $L = m$, respectively, are decoupled. Coupling between the channels occurs if any of the four assumptions (i)–(iv) made in Sec. III is dropped. The generalization of this theory is straightforward but tedious.

The calculated spectrum consists of two parts, a bound state and a continuum $\omega > 2\Delta$. The bound state is formed in the $L \neq 0$ channels for any sign of the coupling and it is orthogonal to the condensed Cooper pair formed with quantum number $L = 0$. The binding energy depends on an effective coupling α_L defined by Eq. (4.4). Even if this coupling may take any value, the most typical ones are around the value 0.1 or they are even smaller. In these cases the binding energy $\omega_{B,L}$ is very small, e.g., $\omega_{B,L}/2\Delta < 0.1$ if the dimensionless BCS coupling $\rho_0 g^* = 0.2$. For $\rho_0 g^* = 0.1$ the binding energy can be even much smaller.

If the bound state has a finite lifetime, then a resonance is formed. If the inverse lifetime or the experimental resolution is larger than the binding energy then the resonance does not split off the continuum. The peak in the spectrum can be below or above 2Δ. In the spectra measured by Hackl[29] or Nb_3Sn, there is a very sharp peak, which may be interpreted as a strong resonance. A close analogy has been established between the present bound states and the two-roton bound states[14–18] in liquid ^{4}He superfluid. In the latter case even for very low temperatures where the roton lifetime is practically infinite, the bound state is not separated from the continuum. As it has been shown, the two-roton resonance has a finite intrinsic lifetime[18] as two rotons with zero total momentum can always decay into a two-phonon state.[30] Similar situations can occur in this case when the excited pair recombines into a Cooper pair (e.g., from state $l = 1$ to $l = 0$) by infrared or two-phonon emission. In Fig. 6 the spectrum measured in V_3Si (Ref. 21) with polarization direction E_g is compared with the curve calculated on the basis of the theoretical formula (4.2) using the parameter values $\alpha_L = 0.5 \times 10^{-3}$, $\Delta = 41$ cm^{-1}, and the Lorentzian width $\Gamma/\Delta = 0.17$ is used to make convolution with the theoretical curve. In this case Δ is also a fitting parameter as precise tunneling data are not available.

The main difficulty with such fitting is that similar

curves can be produced by assuming an anisotropic gap.[20] Polarization dependence can be expected in both cases as in the former case the mixing ratios of different angular momentum channels in the spectrum depend on the polarizations of the light ($\mathbf{e}_i$ and $\mathbf{e}_s$), while in the latter case different Fermi surface regions are dominating.

The dependence of the calculated spectra on the momentum transfer q is weak, but by increasing the momentum transfer the binding energy and the weight of the bound state in the spectrum gradually decreases. As it is pointed out by Abrikosov and Fal'kovsky,[10,24] by increasing q the role of the zero-sound channel decreases because of the appearance of the q-dependent term in the energy denominator. An average over the momentum transfer q results in further smearing of the spectrum.[21,24]

The excited pair with the quantum number $L=0$ but finite q is coupled to the long-range Coulomb field which then screens these excitations almost completely [see Eq. (4.15)]. In the case of mixing of different channels the effect of the Coulomb field can be more complicated.

Considering the high-T_c material $YBa_2Cu_3O_{7-\delta}$ the spectrum with A_{1g} symmetry is very similar to the spectra discussed here,[31,32] but the existence of the low-lying excitations well below the peak suggest a huge anisotropy or alternatively, gapless regions (e.g., nodes). Using the azimuthal quantum number m to characterize the pairs in the quasi-two-dimensional case, the branch with $m=0$ is screened by the Coulomb field but the channel with $m=4$ shows also A_{1g} symmetry. The very different behavior for the B_{1g} symmetry produces further puzzles, and it has been suggested[31,33] that the interband transitions may play a role.

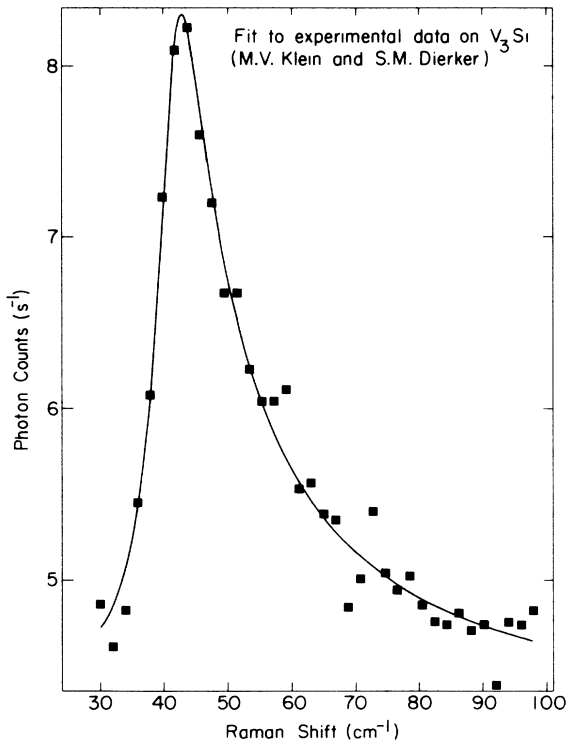

FIG. 6. The experimental Raman intensity measured on V_3Si (Ref. 21) in the E_g symmetry is fitted with theoretical Raman intensity (4.2). The momentum transfer of the light is neglected ($v_F q \sim 0$). The value for the superconducting gap is $2\Delta=41$ cm^{-1}, the broadening is $\Gamma/\Delta=0.17$, and strength of the final-state interaction $\alpha=0.005$.

The role of the electron pair creation and the final-state interaction in phonon dynamics[12,34,21,35,36] has already been studied. In the case of coexistence of charge-density wave (CDW) and superconductivity, Littlewood and Varma[34] pointed out the existence of a combined CDW and superconducting amplitude mode that is electrically neutral; thus it does not couple to the Coulomb field. That mode shows up in the Raman spectra by hybridizing with phonons.

In a recent paper by Zeyher and Zwicknagel[37] studying the electron-phonon interaction in superconductors it is shown that the phonon spectra contains a bound state that is due to the phonon mediated electron-electron interaction in the zero-sound channel; thus it must have excitonic character.

Overdamped excitations in the zero-sound channel may exist in nonsuperconducting solids also, when the electron distribution is rearranged in the momentum space and the long-range charge neutrality is maintained. Such a situation may occur, e.g., in multivalley semiconductors[38,39] and, in principle, in metals also.[40] The overdamped nature may be due to impurity scattering and, in the former case, due to intervalley phonon scattering also. The effect of impurities on the Raman spectra has recently also been discused by Fal'kovsky[41] but only the channel $L=0$ is treated in detail.

In the study of superfluid ^{3}He, collective excitations have been measured by ultrasound absorption.[42] Unfortunately, these studies give detailed information on the collective amplitude modes but up to now much less information is obtained on the continuum.

In summary, a detailed theory of the Raman spectrum is presented for small but finite momentum transfer and for the complete energy interval. The role of the final-state interaction is discussed in great detail. In order to clarify the role of final-state interaction, further careful experimental study of the polarization dependence of the Raman spectra is required and independent measurement of the gap would also be very helpful.

Note added in proof. A fit similar to the one given in Fig. 6 has been made for the V_3Si data of Ref. 21 but for a polarization direction exhibiting $A_{1g}+E_g$ symmetry. The parameters $2\Delta=42$ cm^{-1} and $\Gamma/\Delta=0.15$ are similar but $\alpha=10^{-3}$ is much smaller. That difference is reflecting the different intensities at $\omega \geq 3\Delta$. This polarization dependence of α can be regarded as a *direct evidence for the importance of the final-state interaction.*

ACKNOWLEDGMENTS

The authors are especially grateful to J. Bardeen, M. V. Klein, C. Pethick, and D. Pines for theoretical discussions and to R. Hackl and M. V. Klein for clarifying the experimental situation. The authors also thank P. Fulde and M. Cardona for critical reading of the manuscript. One of the authors (A.Z.) wishes to thank the Science and Technology Center for Superconductivity at the Univer-

sity of Illinois at Urbana-Champaign and the Physics Department at the University of Virginia for their kind hospitality and support. Part of the study was carried out at the Aspen Center for Physics and at the Max-Planck-Institute für Festkörperforschung, Stuttgart. The research also was supported in part by the National Science Foundation (NSF) Grant No. DMR-17613.

APPENDIX A: CALCULATION OF THE SINGLE LOOPS

The Fourier transform of the matrix elements A, B, C, and D are needed in the detailed calculation. The definitions are given by Eqs. (3.9) and (3.10). The Green's functions are given by Eqs. (2.20) and (2.24). The calculation of the simple loop contains one summation over ω_n. The following notation is used:

$$E_{\pm}=(\Delta^2+\xi_{\pm}^2)^{1/2} , \tag{A1}$$

where

$$\xi_{\pm}=\varepsilon_{\mathbf{k}+\mathbf{q}/2}=\xi\pm\mathbf{v}_F\cdot\mathbf{q}/2 . \tag{A2}$$

The integrals over the k spaces are transformed to energy integrals as follows:

$$\frac{1}{(2\pi)^3}\int d^3\mathbf{k}=\rho_0\int d\xi\int\frac{dS}{S_0} , \tag{A3}$$

where a spherical or cylindrical Fermi surface is assumed. In the general case the integral is taken over the weighted Fermi surface element dS/v_F. In this case v_F is constant and S_0 is the area of the Fermi surface. (The difficulty in the calculation is that the product $\mathbf{v}_F\cdot\mathbf{q}$ varies over the Fermi surface.)

The single-loop calculation contains an integral of type (A3), and we list the integrands for A, B, C, and D. Only the even terms in $\mathbf{q}$ are kept because the odd terms drop out in the integration. All the thermal factors are given in the zero-temperature limit.

$$A\rightarrow-\frac{E_++E_-}{2E_+E_-}\frac{\Delta^2-\xi_-\xi_++E_-E_+}{\omega_n^2+(E_++E_-)^2} , \tag{A4}$$

$$B\rightarrow\frac{E_++E_-}{2E_+E_-}\frac{\Delta^2}{\omega_n^2+(E_++E_-)^2} , \tag{A5}$$

$$C\rightarrow\frac{\Delta}{\sqrt{2}E_+E_-}\frac{i\omega_nE_++(E_-+E_+)\xi_+}{\omega_n^2+(E_-+E_+)^2} , \tag{A6}$$

$$D\rightarrow\frac{E_++E_-}{2E_+E_-}\frac{E_+E_-+\xi_+\xi_-}{\omega_n^2+(E_++E_-)^2} . \tag{A7}$$

APPENDIX B: INTEGRALS IN $q=0$ LIMIT

In the quantities A, B, C, and D the analytical calculation is made to the real axis $i\omega_n\rightarrow\omega+i\delta$. The calculation of the integral for finite q is discussed in Appendix C. The results can be expanded as

$$F(\mathbf{q},\omega)=F_0(\omega)+\frac{(\mathbf{q}\cdot v_F)^2}{\Delta^2}\rho_0F_2(\mathbf{q},\omega)+O(q^4) \tag{B1}$$

for $F=A,B,C,D$. The $q=0$ limit can be expressed in terms of the integral I_0 defined by Eq. (4.1) and the gap integral (2.25). The results are

$$A_0=-\tfrac{1}{2}\rho_0I_0(z) , \tag{B2}$$

$$B_0=\tfrac{1}{4}\rho_0I_0(z) , \tag{B3}$$

$$C_0=\frac{1}{4\sqrt{2}}\frac{\omega}{\Delta}\rho_0I_0(z) , \tag{B4}$$

$$D_0=\frac{1}{g^*}+\frac{1}{4}\left[\frac{\omega^2}{2\Delta^2}-1\right]\rho_0I_0(z) , \tag{B5}$$

where $z=1-\omega^2/4\Delta^2$. The function I_0 defined by Eq. (4.1) has the following analytical forms:

$$I_0(z)=\begin{cases}\dfrac{2}{\sqrt{z(1-z)}}\arcsin\sqrt{1-z}, & 0\le z\le 1 \quad \text{(B6a)}\\ \dfrac{2}{\sqrt{z(z-1)}}\arcsin\sqrt{z-1}, & 1\le z \quad \text{(B6b)}\\ -\dfrac{2}{\sqrt{-z(1-z)}}\arcsin\sqrt{-z}+\dfrac{i\pi}{\sqrt{-z(1-z)}}, & z<0 . \quad \text{(B6c)}\end{cases}$$

APPENDIX C: CALCULATION OF FUNCTIONS A, B, C, AND D FOR SMALL q

In the following calculations integrals of type

$$I_n(z)=\int_{-\infty}^{\infty}\frac{1}{(1+x^2)^{n+1/2}}\frac{1}{z+x^2}dx \tag{C1}$$

appear. The integral $I_0(z)$ has already been given by Eq. (4.1) and expressed by Eqs. (B6a)–(B6c). The integrands of the integrals with $n=1,2$ can be expressed by the function $I_0(z)$ due to recursion equations as

$$I_1(z)=\frac{1}{1-z}[-2+I_0(z)] \tag{C2a}$$

and

$$I_2(z)=\frac{1}{1-z}\left[-\frac{4}{3}-\frac{2}{1-z}+\frac{1}{1-z}I_0(z)\right] . \tag{C2b}$$

The functions $A(q,\omega)$, $B(q,\omega)$, $C(q,\omega)$, and $D(q,\omega)$ can be obtained by the analytical continuation of expressions (A4)–(A7) by replacing $\omega_n^2\rightarrow-\omega^2$, thus, for example, the function $A(q,\omega)$ is

$$A(q,\omega)=\rho_0\int d\xi\int\frac{dS}{S_0}\frac{E_++E_-}{2E_+E_-}\frac{\Delta^2-\xi_-\xi_++E_+E_-}{(E_++E_-)^2-\omega^2}\ ,$$

where the notations given by Eqs. (A1)–(A3) are introduced.

The next step is the expansion in $(\mathbf{v}_F\mathbf{q})/\Delta$ that leads to

$$\frac{1}{(E_++E_-)^2-\omega^2}=\left[\frac{1}{4}+\frac{(\mathbf{v}_F\cdot\mathbf{q})^2\Delta^2}{\omega^4}\right]\frac{1}{\Delta^2+\xi^2+(\mathbf{v}_F\cdot\mathbf{q})^2\Delta^2/\omega^2-\omega^2/4}-\frac{(\mathbf{v}_F\cdot\mathbf{q})^2\Delta^2}{\omega^2}\frac{1}{\Delta^2+\xi^2-(\mathbf{v}_F\cdot\mathbf{q})^2\Delta^2/\omega^2}\ , \tag{C3}$$

$$\frac{E_-+E_+}{2E_-E_+}=\frac{1}{E}+\frac{1}{4}\frac{(\mathbf{v}_F\cdot\mathbf{q})^2}{E^3}-\frac{3}{8}\frac{(\mathbf{v}_F\cdot\mathbf{q})^2\Delta^2}{E^5}+\cdots\ , \tag{C4}$$

and

$$\frac{1}{E_-}=\frac{1}{E}+\frac{1}{4E^3}(\mathbf{v}_F\cdot\mathbf{q})^2-\frac{3}{8}\frac{\Delta^2}{E^5}(\mathbf{v}_F\cdot\mathbf{q})^2\ , \tag{C5}$$

where the terms odd in ξ are not written out, because they will drop out in the integration; furthermore,

$$\xi_+\xi_-=\xi^2-\tfrac{1}{4}(\mathbf{v}_F\mathbf{q})^2\ , \tag{C6}$$

$$E_+E_-=E^2\left[1+\tfrac{1}{4}(\mathbf{v}_F\mathbf{q})^2\frac{\Delta^2-\xi^2}{E^4}\right]\ , \tag{C7}$$

$$E_++E_-=2E+\tfrac{1}{4}(\mathbf{v}_F\mathbf{q})^2\frac{\Delta^2}{E^3}\ . \tag{C8}$$

The integrals with respect to ξ can be expressed in terms of the functions I_n $(n=0,1,2)$. By taking the average over the Fermi surface of the expansion given by Eq. (B1) for function $F=A,B,C,D$ the following form is obtained:

$$F(\mathbf{q},\omega)=\int\frac{dS}{S_0}F(\mathbf{q},\omega)=F_0(\omega)+\rho_0\int\frac{dS}{S_0}\frac{(\mathbf{q}\cdot\mathbf{v}_F)^2}{\Delta^2}F_2(\mathbf{q},\omega)\ . \tag{C9}$$

The result of a straightforward algebra is

$$A_2(\mathbf{q},\omega)=-\tfrac{1}{4}I_1(z)+\tfrac{3}{16}I_2(z)-J\ , \tag{C10}$$

$$B_2(\mathbf{q},\omega)=\tfrac{1}{4}I_0(z)-\tfrac{3}{8}I_2(z)-2J\ , \tag{C11}$$

$$C_2(\mathbf{q},\omega)=\frac{1}{2\sqrt{2}}\left[\frac{\omega}{2\Delta}\right][\tfrac{1}{8}I_1(z)-\tfrac{3}{16}I_2(z)+J]\ , \tag{C12}$$

$$D_2(\mathbf{q},\omega)=\tfrac{1}{2}A_2(\mathbf{q},\omega)\ , \tag{C13}$$

$$J=\tfrac{1}{8}\left[\frac{2\Delta}{\omega}\right]^4[I_0(z)-I_0(z')]\ , \tag{C14}$$

where $z=1+s^{-2}\mu^2-\omega^2/4\Delta^2$ and $z'=(1-s^{-2}\mu^2)$ with the notations $\mu=(\mathbf{v}_F\cdot\mathbf{q})/(vq)$ and $s^{-1}=v_Fq/\omega$. The gap integral is expressed by the coupling g^* [see Eq. (2.25)].

Abrikosov and Fal'kovskii[24] studied the region $2\Delta<\omega\ll 2\Delta\{1+(qv_F)^2]^{1/2}$ [case (i)] with special care. The functions I_0 with variable z' have regular behavior for $v_Fq/\omega=s^{-1}\mu\ll 1$ as the function I_0 given by Eq. (B6a) is regular at $z'=1$.

In the functions I_n with variable z, however, there are singularities because the integrals that define these functions are taken over a singular expression [see the discussion following Eq. (4.7)]. The singular behavior occurs around $z=0$ or $\omega^2=4\Delta^2[1+(\mathbf{q}\cdot\mathbf{v}_F)^2/\omega^2]$, and because of Eqs. (C2a) and (C3b) the strengths of the singularities are determined by function $I_0(z)$. In the region studied by Abrikosov and Fal'kovskii[24] the pole occurs for $\mu^2\ll 1$. For larger μ^2 values the argument of the function I_0 can be approximated by

$$s^{-2}\mu^2\sim(v_Fq)^2\mu^2/(4\Delta^2)\ll 1\ .$$

According to Eq. (B6a) there is a singularity like $(q\mu)^{-1}$ in function I_0. In dimension $d=3$ with spherical Fermi surface, the integral with respect to $d\mu$ results in a logarithmic term $\ln(v_Fq\mu)/v_Fq$. As the preceding approximation is not valid for small μ, therefore, a lower cutoff must be applied in the energy range $v_Fq\mu\sim[\omega^2/(4\Delta^2)-1]^{1/2}$. The upper limit of the integral is $\mu=1$, thus the contribution is proportional

$$\frac{\Delta}{v_Fq}\ln\frac{v_Fq}{(\omega^2/4\Delta^2-1)^{1/2}}\gg 1\ ,$$

which is not singular in q for small ω, as the very small q values are excluded from the region studied. That result holds for the real part.

The imaginary part, however, is restricted to the small μ^2 values where Eq. (B6c) holds. In this case the argument of function I_0 can be approximated by $(\omega^2/4\Delta^2-1)$. The interval of the integration with respect to μ is proportional to $(\omega^2/4\Delta^2-1)^{1/2}(v_Fq)$, thus the result is proportional to $\Delta/(v_Fq)\gg 1$. Furthermore, the most singular part of the final expression of the imaginary part of the function π^{00} is proportional to the imaginary part and the inverse of the square of the real part of I_0. That is the origin of the

$$q\ln^{-2}\left[\frac{(v_Fq)^2}{\omega^2/(4\Delta^2)-1}\right]^{1/2}$$

behavior. In the channel $L=0$ with the additional q^2 term the result given in Eq. (17) in Ref. 24 can be obtained. It must be emphasized that in Ref. 24 the Coulomb field is not treated.

Finally, it is worthwhile to point out that in region III the $q\to 0$ limit can be taken as the variable z remains finite.

*Permanent address: Institute of Theoretical Physics, Eötvös Roland University, H-1088 Budapest, Puskin u. 5-7, Hungary.

[1]J. Bardeen, L. N. Cooper, and J. R. Schrieffer, Phys. Rev. **108**, 1175 (1957).

[2]P. W. Anderson, Phys. Rev **112**, 1900 (1958).

[3]P. W. Anderson, Phys. Rev. **110**, 827 (1958).

[4]N. N. Bogoliubov, Nuovo Cimento **7**, 6 (1958); **7**, 794 (1958); N. N. Bogoliubov, V. V. Tolmachev, and D. V. Shirkov, *A New Method of the Theory of Superconductivity* (Consultants Bureau, New York, 1959).

[5]T. Tsuneto, Phys. Rev. **118**, 1029 (1960).

[6]A. Bardasis and J. R. Schrieffer, Phys. Rev. **121**, 1050 (1961); see also V. G. Vaks, V. M. Galitskii, and A. I. Larkin, Zh. Eksp. Teor. Fiz. **41**, 1655 (1961) [Sov. Phys.—JETP **14**, 1177 (1962)].

[7]K. Maki and T. Tsuneto, Prog. Theor. Phys. (Kyoto) **28**, 163 (1962); P. Fulde and S. Strassler, Phys. Rev. **140**, A519 (1965).

[8]For a general discussion, see P. C. Martin, in *Superconductivity,* edited by R. D. Parks (Dekker, New York, 1969), Vol. 1, p. 37.

[9]See, e.g., P. Wölfle, in *Progress in Low Temperature Physics,* edited by D. F. Brewer (North-Holland, Amsterdam, 1987). The excitations with higher angular momenta are discussed by J. A. Sauls and J. W. Serine, Phys. Rev. B **23**, 4798 (1981).

[10]A. A. Abrikosov and L. A. Fal'kovsky, Zh. Eksp. Teor. Fiz. **40**, 262 (1961) [Sov. Phys.—JETP **13**, 179 (1961)].

[11]S. Y. Tong and A. A. Maradudin, Mater. Res. Bull. **4**, 563 (1969).

[12]R. Sooryakumar and M. V. Klein, Phys. Rev. Lett. **45**, 660 (1980); Phys. Rev. B **23**, 3213 (1981); R. Sooryakumar, M. V. Klein, and R. F. Frindt, *ibid.* **23**, 3222 (1981).

[13]J. Bardeen (private communication).

[14]T. J. Greytak and J. Yan, Phys. Rev. Lett. **22**, 987 (1969); T. J. Greytak, R. Woerner, J. Yan, and R. Benjamin, *ibid.* **25**, 1547 (1970); for a review, see T. J. Greytak, in *Quantum Liquids,* edited by J. Ruvalds and T. Regge (North-Holland, New York, 1978), p. 121.

[15]J. Ruvalds and A. Zawadowski, Phys. Rev. Lett. **25**, 333 (1970); for a review, see A. Zawadowski, in *Quantum Liquids,* edited by J. Ruvalds and T. Regge (North-Holland, New York, 1978), p. 293.

[16]F. Iwamoto, Prog. Theor. Phys. (Kyoto) **44**, 1121 (1970).

[17]A. Zawadowski, J. Ruvalds, and J. Solana, Phys. Rev. A **5**, 399 (1972).

[18]C. A. Murray, R. L. Woerner, and T. J. Greytak, J. Phys. C **8**, L90 (1975).

[19]A. D. B. Woods, P. A. Hilton, R. Scherm, and W. G. Sterling, J. Phys. C **10**, L45 (1977).

[20]S. B. Dierker, M. V. Klein, G. W. Webb, and Z. Fisk, Phys. Rev. Lett. **50**, 853 (1983).

[21]M. V. Klein and S. B. Dierker, Phys. Rev. B **29**, 4976 (1984).

[22]M. V. Klein, in *Superconductivity in d- and f-Band Metals,* edited by W. Buckel and W. Weber (Kernforschungszentrum Karlsruhe, Karlsruhe, 1982), p. 539; S. B. Dierker, M. V. Klein, G. Webb, Z. Fisk, J. Wernick, G. Hull, J.-E. Jörgensen, and S. R. Rasmussen, *ibid.*, p. 563.

[23]R. Hackl, R. Kaiser, and S. Schicktanz, in *Superconductivity in d- and f-Band Metals,* Ref. 22, p. 539; R. Hackl, R. Kaiser, and S. Schicktanz, J. Phys. C **16**, 1729 (1983).

[24]A. A. Abrikosov and L. A. Fal'kovsky, Physica C **156**, 1 (1988).

[25]A. A. Abrikosov and V. M. Genkin, Zh. Eksp. Teor. Fiz. **65**, 842 (1973) [Sov. Phys.—JETP **38**, 417 (1974)].

[26]A. A. Abrikosov, L. P. Gorkov, and I. E. Dzyaloshinski, *Methods of Quantum Field Theory in Statistical Physics* (Dover, New York, 1963).

[27]K. Bedell, D. Pines, and A. Zawadowski, Phys. Rev. B **29**, 102 (1984).

[28]K. Ohbayashi, T. Akagi, N. Ogita, M. Watabe, and M. Udagawa, Jpn. J. Appl. Phys. **26**, 5 (1987).

[29]R. Hackl, doctoral thesis, Technische Universität, München, 1987 (unpublished).

[30]R. L. Woerner and M. J. Stephen, J. Phys. C **8**, L464 (1975).

[31]S. L. Cooper, M. V. Klein, B. G. Pazol, J. P. Rice, and D. M. Ginsberg, Phys. Rev. B **37**, 5920 (1988).

[32]S. L. Cooper, F. Slakey, M. V. Klein, J. P. Rice, E. D. Bukowski, and D. M. Ginsberg, Phys. Rev. B **38**, 11 934 (1988); F. Slakey, S. L. Cooper, M. V. Klein, J. P. Rice, and D. M. Ginsberg, *ibid.* **39**, 2781 (1989), S. L. Cooper, F. Slakey, M. V. Klein, J. P. Rice, E. D. Bukowski, and D. M. Ginsberg, J. Opt. Soc. Am. B **6**, 436 (1989); R. Hackel, W. Gläser, P. Müller, D. Einzel, and K. Andres, Phys. Rev. B **38**, 7133 (1988); T. Ruf, C. Thomsen, R. Liu, and M. Cardona, *ibid.* **38**, 11 985 (1988).

[33]H. Monien and A. Zawadowski, Phys. Rev. Lett. **63**, 911 (1989).

[34]P. B. Littlewood and C. M. Varma, Phys. Rev. Lett. **47**, 811 (1981); Phys. Rev. B **26**, 4883 (1982); see also D. A. Browne and K. Levin, Phys. Rev. B **2**, 4029 (1982).

[35]C. A. Balserio and L. M. Falicov, Phys. Rev. Lett. **45**, 662 (1980).

[36]D. A. Browne and K. Levin, Phys. Rev. B **28**, 4029 (1983).

[37]R. Zeyher and G. Zwicknagel, Z. Phys. B **78**, 175 (1990).

[38]G. Contreras, A. K. Sood, and M. Cardona, Phys. Rev. B **32**, 924 (1985); *ibid.* **32**, 930 (1983).

[39]See, for theory, S. V. Gantsevich, R. Katilyus, and N. G. Ustinov, Fiz. Tverd. Tela **16**, 1106 (1974) [Sov. Phys.—Solid State **16**, 711 (1974)] and I. P. Ipatova, A. V. Subashiev, and V. Voitenko, Solid State Commun. **37**, 893 (1981).

[40]M. Cardona and A. Zawadowski (unpublished).

[41]L. A. Fal'kovsky, Zh. Eksp. Teor. Fiz. **95**, 1146 (1989) [Sov. Phys.—JETP **68**, 661 (1989)].

[42]See, e.g., B. S. Shivaram, M. W. Meisel, K. Bimel, K. Sarma, W. P. Halperin, and J. B. Ketterson, Phys. Rev. Lett. **50**, 1070 (1583).